

Remote mass facial temperature screening in varying ambient temperatures and distances

Chu Chu Qiu¹, Jing Wei Chin², Kwan Long Wong^{1,2}, Tsz Tai Chan², Yu Dong He¹, Richard H.Y. So^{1,2}

¹ The Hong Kong University of Science and Technology ² PanopticAI Ltd.

Abstract

Remote body temperature measurement using infrared thermography has been widely deployed worldwide to detect feverish persons, but the measurement accuracy is affected by various factors including ambient temperature and sensor-subject distance. We present a novel compensation model to address the undesirable interacting influence of ambient temperature and sensor-subject distance during remote facial temperature screening in real-world setting. We derived our model on site-data collected over 12 months and demonstrated the significant linear relationship between ambient temperature and the measured temperature from a thermal camera. In addition, the interaction between the effects of sensor-subject distance and ambient temperature on the measured temperature is significant. Our model can significantly reduce the measurement error (MAE) by 23.5% and is better than the best existing models. The model can also extend the detection distance by up to 46% with sensitivity and specificity over 90%.

1. Introduction

Temperature is one of the most important vital signs for health monitoring. The remote mass facial temperature screening system, which can be placed far without obstructing pedestrians, has been widely used to screen for feverish persons since the outbreak of SARS [2, 20]. These systems, equipped with both color and thermal cameras, can detect the facial temperatures of multiple persons simultaneously in a contactless manner, thereby enabling the identification of potentially infected people at an early stage. In the wake of the COVID-19 outbreak, the systems were installed not only at national borders but also at the entrances of various venues to prevent feverish from accessing public indoor areas. The integration of thermal screening into security solutions has become an important measure to safeguard public health in the most relevant ways. Nevertheless, the fluctuating ambient temperature may lead to an inaccurate body

temperature measurement, which is not in compliance with the Food and Drug Administration's guidelines [13] that suggest the temperature screening system to be operated in an environment of 20°C to 24°C. This leads to the question we are trying to solve in this paper: How to accurately detect persons with elevated body temperature under a wide range of distances and varying ambient temperatures using infrared thermography?

Since accurate temperature measurement is the foundation of remote temperature measurement using infrared thermography, therefore, our focuses are: (i) the effect of ambient temperature on the measured temperature, (ii) the interaction between distance effects and ambient temperature effects on the measured temperature, (iii) a more comprehensive compensation model that takes not only distance between the camera and the subject (sensor-subject distance) and ambient temperature but also their interactions into account, which is tested in a public area. Our study provides a comprehensive analysis of the effects of both distance and ambient temperature on the measured temperature in a public environment. Below is a summary of our contributions.

1. Our results show that the maximum measured facial temperature increases significantly ($p < 0.01$) and linearly as the ambient temperature increases.
2. Our results show that there is an interaction effect between sensor-subject distance and ambient temperature ($p < 0.01$).
3. With our proposed compensation model, our results show that the system detects febrile persons successfully with sensitivity and specificity over 90%. The maximum detection range is 6 m (the whole detection area) in ambient temperatures ranging from 28.6°C to 29°C.

2. Related Works

Infrared thermography has proven to be an effective method for measuring human body temperature [5]. Since

the SARS outbreak in 2003, infrared thermography has been widely utilized in temperature screening, particularly in airports and international borders. [4, 11, 12, 15, 20]. Generally, a traditional facial temperature screening system would notify border control personnel when a person with an abnormal temperature passes through the checkpoint. The staff would then manually compare images taken from the thermal and color cameras in the system to pinpoint the target person, and they would promptly stop the suspect before they could depart the screening area. The procedure requires a great deal of work and puts enormous strain on personnel, as it needs to be finished swiftly. With the introduction of deep learning and AI in computer vision area [3, 18], there has been a surge in the development of more intelligent systems [7, 10, 16, 21] for facial temperature screening applications.

Precise measurement of human body temperature using a thermographic camera is crucial for detecting people with abnormal body temperature with automated mass facial temperature screening systems. Several studies investigated the impact of different factors on temperature measurement with a thermographic camera, including the presence of dust [14], wind velocity [23], the ambient temperature [17, 19, 23], the distance between the camera and the subject [7, 9], and so on. Pan et al. evaluated the effect of dust on temperature measurements [14]. Wind and heating, on the other hand, can significantly influence temperature measurement, as demonstrated in experiments with black bodies at 35°C and 55°C [23]. Nonetheless, as this study’s focus does not encompass the investigation of dust, wind, and heating effects on temperature measurement, these factors were not simulated.

The effects of ambient temperature on the measured temperature have been highlighted as a significant factor in several studies [17, 23]. However, as for the relationship between ambient temperature and the measured temperature, there is a contradiction in Wan’s finding [23] and Vuttyvong’s [17]. Wan et al. [23] found a linear relationship between ambient temperature, while Vuttyvong et al. [17] thought it was a quadratic relationship. To apply the mass temperature screening system in varying ambient temperatures, we focus on exploring the relationship between ambient temperature and the measured temperature in the field study. The effect of distance and ambient temperature on the measured temperature would interact, and to have precise body temperature detection in a wide range of distances and ambient temperatures, this factor cannot be neglected. However, the interaction between the effects of distance and ambient temperature on the measured temperature has not been explored in the mass facial temperature screening system [7, 8, 16, 17, 21].

To mitigate the noise of temperature measurement caused by different factors, in previous studies Zhang et

al. [9] made theoretical corrections related to distance and Chin et al. [7] proposed a compensation model only considering the distance factor after finding the significant linear relationship between the distance and the measured temperature. Additionally, Vuttyvong et al. [17] proposed two compensation models, independently considering the distance and ambient temperature. The authors of [8] demonstrated a compensation model using a neural network that only considers distance at 1 meter and 2 meters, yet the experiment they conducted was not sufficiently regulated. In conclusion, no compensation model accounts for the effects of ambient temperature, distance, and their interactions on the measured temperature. Consequently, our paper focuses on studying the relationship between ambient temperature and the measured temperature, the interaction between the effects of ambient temperature and distance on the measured temperature, and the compensation model.

3. Methods

To facilitate our study, we implemented an remote mass facial temperature screening system [7] at a commercial site, as demonstrated in Figure 1. It consists of a distinct camera setup featuring a Logitech BRIO color camera, a FLIR E6 thermal camera, an environmental sensor, and a PC for computing.

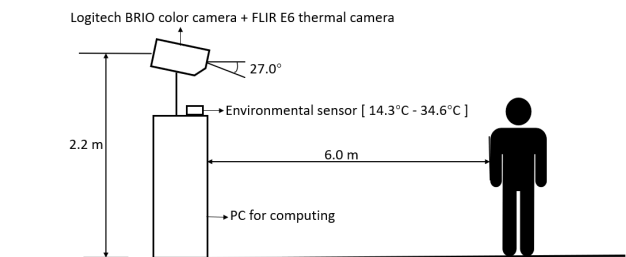


Figure 1. Schematic diagram of the flow of collecting data with the remote mass facial temperature screening system

3.1. Data information

We collected a private dataset that consists of key-point information from the human body extracted with OpenPose [3] and thermal faces (a 2D temperature array of a face shown in Figure 4) with the above-mentioned system. They were collected in a field site that is sheltered outdoors from June 2021 to June 2022. The raw dataset consists of 23,371,717 data points. Since the site’s furthest distance is 6 meters, we only collected data from 0.25 m to 6 m. Figure 2 demonstrates the variation of humidity and ambient temperature during the data-gathering period between June 2021 and June 2022. The environmental temperature range is between 14.3°C and 34.6°C. The mean and standard deviation are 27.7°C and 3.7°C, respectively. Furthermore,

the humidity range is between 25.6% and 94.1%. The mean and standard deviations are 65.8% and 11.4%, respectively.

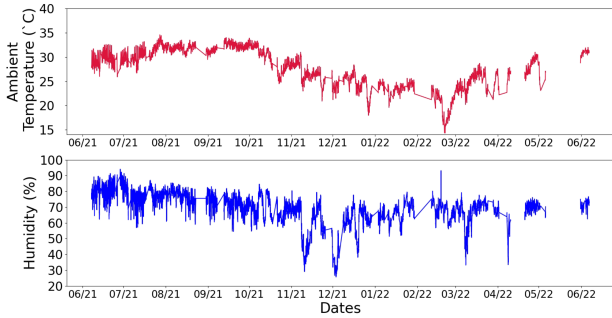


Figure 2. Data information: Change of Ambient Temperature and Humidity from Jun 2021 to Jun 2022. The Ambient temperature ranges from 14.3°C to 34.6°C and the Humidity ranges from 25.6% to 94.1%.

To have an accurate sensor-subject distance estimation and compensation on the measured temperature measured by the thermal camera, we also collected calibration data, including non-fever data and simulated fever data with extra reference forehead temperature measured by a handheld thermometer (HuBDIC Non-Contact infrared Thermometer FS-300). Similar to a previous study [7], a hot pack was put on the subject’s forehead for 10 seconds before the temperature measurement to simulate fever. The range of referenced normal temperature is between 36.4°C and 36.5°C. The range of referenced fever temperature is between 38.2°C and 38.3°C. The range of the ambient temperature is from 28.7°C to 29°C. The mean and standard deviation of the ambient temperature are 28.8°C and 0.1°C, respectively. The range of the humidity is from 72.5% to 73%. The mean and standard deviation of the humidity are 72.9% and 0.1% during the calibration period.

3.2. Distance estimation

Since the remote mass facial temperature screening system does not have a depth sensor, the sensor-subject distance is approximated through the average of the diagonal length of the face boxes using Equation 1 [7], where d denotes the sensor-subject distance, f denotes the average of the diagonal length of the face boxes, and a , b , and c denote the coefficients of the functions.

$$d = \frac{a}{f + b} + c \tag{1}$$

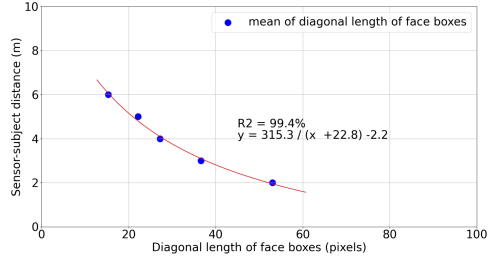


Figure 3. Plot of the sensor-subject distance versus the average of the diagonal length of the face boxes of the calibration subject. The sensor-subject distance and the average of the diagonal length of the face boxes are highly correlated ($R^2 = 99.4\%$).

Figure 3 shows the relationship between the sensor-subject distance and the average of the diagonal length of the face boxes. The subject was filmed head-on at 1-meter intervals between 2 and 6 meters, and the parameters a , b , and c were determined to be 315.3, 22.8, and -2.2, respectively.

3.3. Data Processing

Since Zhou et al. [24] suggested that the maximum temperature of a whole face is an effective alternative for temperature screening, we applied a series of condition filters listed in Table 1 to obtain a full frontal thermal face (e.g. Figure 4) for our analysis. There are four major filtering criteria: (i) To obtain data within the valid distance, (ii) To obtain data at the valid temperature, (iii) To obtain full thermal faces (iv) To obtain front-facing thermal faces. In addition to the four filters, humidity is controlled within 60% to 80% to match the humidity of the calibration data for further study. After the filtering, $N = 20,471$ data points remained in our clean dataset out of the 23,371,717 data points in the raw dataset. Figure 5 illustrates the distribution of data after data cleaning, with regards to both ambient temperature and humidity, indicating that the ambient temperature of the majority of the data (94.3%) exceeds the FDA-suggested ambient temperature range. The environmental temperature is ranging from 15.9°C to 34.4°C. The mean and standard deviation are 29.6°C and 2.9°C, respectively. As mentioned above, the range of humidity is between 60% and 80%. The mean and standard deviation are 71.3% and 5.5%, respectively.

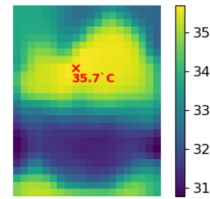
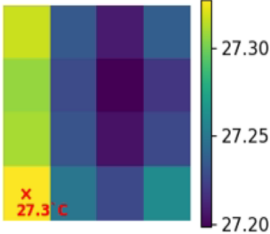
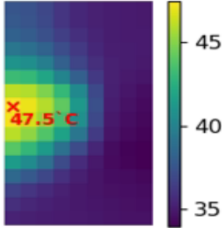
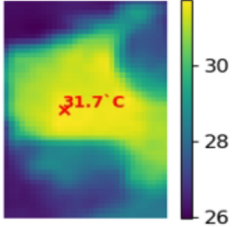
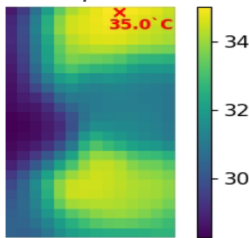


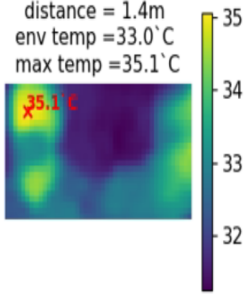
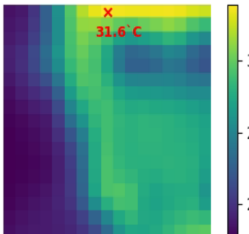
Figure 4. An example of the thermal image of a face facing the camera. The maximum measured facial temperature is 35.7°C.

Table 1. Filtering criteria applied to extract a full frontal thermal face from the raw measured images. After filtering, N = 20,471 data points remained in our clean dataset out of the 23,371,717 data points in the raw dataset.

Filter name	Description	Criteria	Discarded example
Criteria 1: To obtain data in valid distance			
Distance Filter	<ul style="list-style-type: none"> To filter out the invalid distances that exceed the physical location which can be caused by errors due to sensor-subject distance estimation 	<ul style="list-style-type: none"> 0.25 - 6 m 	<p>distance = 8.1m env temp = 30.3 °C max temp = 27.3 °C</p> 
Criteria 2: To obtain data in valid temperature			
Temperature Filter	<ul style="list-style-type: none"> To filter out invalid temperatures caused by the wrong estimation by the thermal camera such as the temperature over 100°C 	<ul style="list-style-type: none"> Valid temperature is within (20°C, 40°C) Valid body temperature is higher than the environmental temperature The definition of valid temperature is the range of body temperature measured by the thermal camera which can be affected by multiple factors. 	<p>distance = 4.6m env temp = 33.6 °C max temp = 47.5 °C</p> 
Criteria 3: To obtain front-facing thermal faces			
Head Orientation Filter	<ul style="list-style-type: none"> To filter out lateral faces 	<ul style="list-style-type: none"> Key-point confidence [3] of the left and right eyes > 0.75 Key-point confidence of the left and right ears > 0.5 Key-point confidence difference in left and right ears < 0.05 	<p>distance = 1.2m env temp = 27.9 °C max temp = 31.7 °C</p> 
Criteria 4: To obtain full thermal faces			
Central face Filter	<ul style="list-style-type: none"> To retain thermal faces with the hottest pixel in the center where the hottest pixel is normally located on the forehead or the inner canthi. 	<ul style="list-style-type: none"> The hottest pixel on the face is not on the edges (within 40% center left-right and 50% top-bottom and starting from 20% from the top) 	<p>distance = 3.0m env temp = 30.4 °C max temp = 35.0 °C</p> 

Continued on next page

Table 1 – continued from previous page

Filter name	Description	Criteria	Discarded example
Valid Face Filter	<ul style="list-style-type: none"> To filter out the extremely long and short faces because Open-pose may wrongly recognize two faces as one 	<ul style="list-style-type: none"> The ratio of the color face is within (0.8, 2) The ratio of the thermal face is within (0.8, 2) <ul style="list-style-type: none"> The definition of face ratio: The height of the face divided by the width of the face 	<p>distance = 1.4m env temp = 33.0°C max temp = 35.1°C</p> 
Forehead Filter	<ul style="list-style-type: none"> To retain face showing forehead 	<ul style="list-style-type: none"> Percentage of the pixels with temperature between peak temperature – 1.5°C and peak temperature > 0.1 	<p>distance = 3.6m env temp = 25.1°C max temp = 31.6°C</p> 

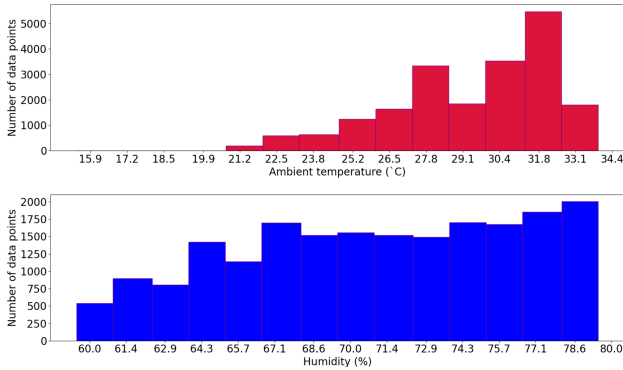


Figure 5. Data distribution of the dataset after data cleaning regarding ambient temperature and humidity. The ambient temperature of 94.3% of the data after cleaning exceeds the FDA-suggested ambient temperature range.

3.4. Compensation model

Ever since the outbreak of COVID-19, many facial temperature screening systems have been installed at locations with varying ambient temperatures which may not follow the suggested environmental temperature of between 20°C and 24°C [13]. This can cause inaccurate temperature measurement and eventually causes imprecise fever detection. After exploring the effect of both ambient temperature and sensor-subject distance on the measured temperature (results in section 4.1 and 4.2), we extend the compensation formula [7] by including ambient temperature, the sensor-subject distance and their interactions which can be defined

by Equation 2.

$$T'_m = T_m + a_1D + a_2T_{amb} + a_3D * T_{amb} + a_4 \quad (2)$$

where T'_m denotes the Compensated Measured Temperature
 T_m denotes the Measured Temperature
 D denotes the Sensor-subject Distance
 T_{amb} denotes the Ambient Temperature
 $D * T_{amb}$ denotes the interaction between the effects of Sensor-subject Distance and Ambient Temperature
 a_n denote the coefficients of the factors, where $n \in 1, 2, 3, 4$

3.5. Metrics

Mean Absolute Error (MAE) and Root Mean Square Error (RMSE) are used to compare the compensated measured temperature and reference temperature. We further evaluated the accuracy of the compensation model through a sensitivity and specificity assessment. The analysis could evaluate the effectiveness of the compensation on fever detection. The equations shown in Equation 3 and Equation 4 illustrate the definition of sensitivity and specificity.

$$Sensitivity = \frac{TP}{TP + FN} \quad (3)$$

where TP denotes the number of fever persons correctly regarded as fever
 FN denotes the number of fever persons incorrectly regarded as non-fever

$$Specificity = \frac{TN}{TN + FP} \quad (4)$$

where TN denotes the number of non-fever persons correctly regarded as non-fever

FP denotes the number of non-fever people incorrectly regarded as fever

4. Results

4.1. Ambient effect

$N = 20,471$ measurements of the data from our clean dataset were filtered at different distances (0.25 m to 6 m). Figure 6 illustrates the measured temperature obtained at different ambient temperatures. The field data demonstrates a statistically significant linear rise in the maximum measured facial temperature as the ambient temperature increased ($p < 0.01$). The finding is consistent with [23].

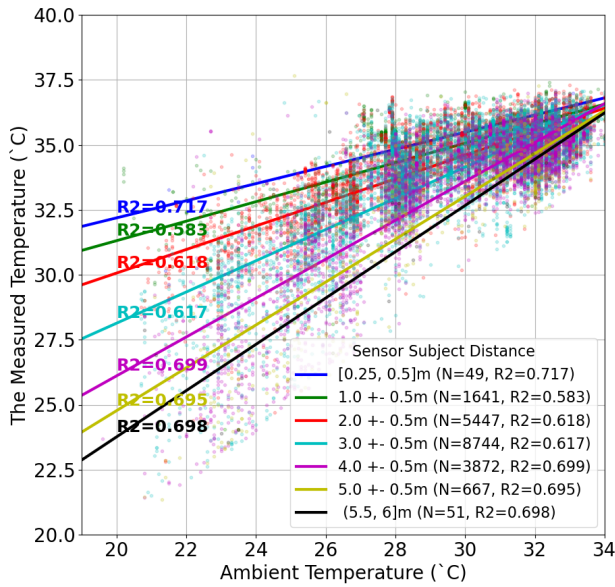


Figure 6. Temperature Measurement over Sensor subject Distance. A significant linear relationship between Ambient Temperature and The Measured Temperature over different distances from 0.25 m to 6 m ($N = 20471$)

4.2. Interaction effect

The Interaction effect was explored to see whether the effects of sensor-subject distance and ambient temperature on the measured temperature interact. The result indicates that as the distance increased, the maximum facial temperature linearly decreased ($p < 0.01$). Additionally, the ambient temperature led to a significantly greater decrease ($p < 0.01$) in temperature, with the measured temperature

dropping faster as ambient temperature decreased. In short, the evidence suggested a significant correlation ($p < 0.01$) between the effects of sensor-subject distance and ambient temperature on the measured temperature.

4.3. Compensation model

We incorporated sensor-subject distance, ambient temperature, and their interactions into our proposed compensation model. 90:10 split on our clean dataset was used for training and testing, respectively. The coefficients in Equation 2 were determined by leveraging the Optimization, and Root finding capabilities of the Scipy library [22]. Due to practical limitations, it was not feasible to measure the reference temperature of all passersby with a handheld thermometer. As a result, a referenced temperature of 36.5°C was adopted as the referenced temperature for non-fever data points in the field data. The compensated temperature was then plotted against different ambient temperatures, as depicted in Figure 7.

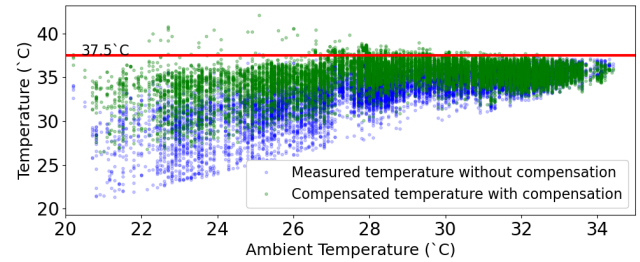


Figure 7. Temperature Measurement over Ambient temperature. The measured temperature and the compensated temperature after correction under different ambient temperatures

Table 2 provides a comparison between the measured temperature (i) without temperature compensation, (ii) with the ambient temperature compensation, (iii) with sensor-subject distance compensation, and (iv) with our proposed compensation and referenced temperatures. Evaluation of the models is based on two metrics, MAE and RMSE. The result shows that the MAE and RMSE between measured temperatures before compensation and referenced temperatures are 2.5°C and 3.3°C , respectively. When compensation was only applied to compensate for the ambient effect, the MAE and RMSE dropped to 1.7°C and 2.5°C . Similarly, the MAE and RMSE attained the values of 1.7°C and 2.6°C with compensation only with sensor subject distance effect. Our newly proposed compensation model demonstrated a reduction in the MAE and RMSE, decreasing to 1.3°C and 1.8°C , respectively. These values significantly reduced ($p < 0.01$) the MAE and RMSE by 23.5% and 28% respectively, compared to the compensation model only with ambient effect. In addition, our compensation model also exhibited a statistically significant reduction (p

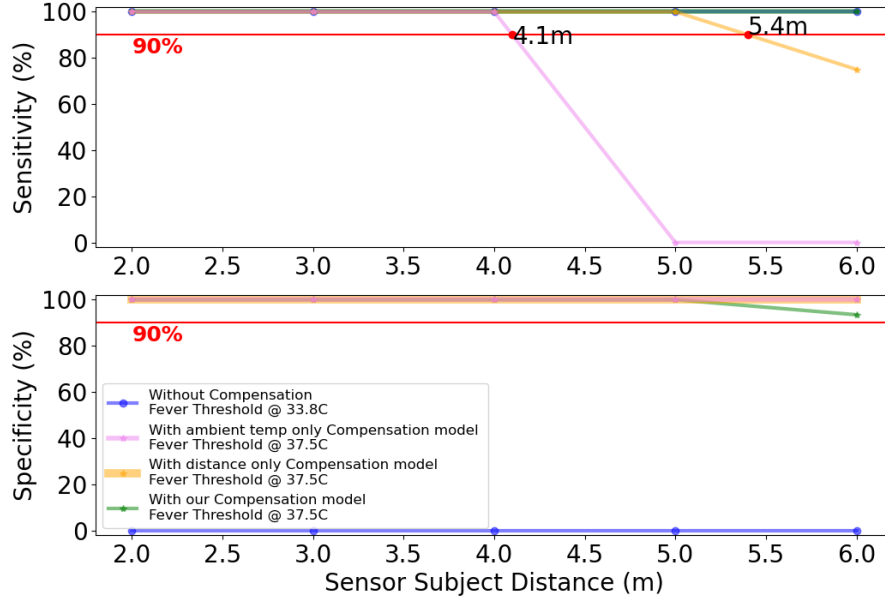


Figure 8. Sensitivity and specificity analysis among different compensation models and without compensation from 2 m to 6 m. The valid detection distance can reach 6 m (the whole area) at a sensitivity and specificity of 90%.

Table 2. Comparison of the average Mean Absolute Error (MAE), and average Root Mean Square Error (RMSE) between different compensation models

Models	Training data (N = 18436)		Testing data (N = 2049)	
	MAE (°C)	RMSE (°C)	MAE (°C)	RMSE (°C)
Measured Temperature	2.5	3.4	2.5	3.3
Compensated Temperature (Distance Only)	1.7	2.6	1.7	2.6
Compensated Temperature (Ambient Temperature Only)	1.7	2.6	1.7	2.5
Compensated Temperature (Distance + Ambient Temperature + Interaction between Distance effect and Ambient Temperature effect)	1.3	1.8	1.3	1.8

< 0.01) of 0.4°C and 0.8°C in MAE and RMSE, reducing by 23.5% and 30% respectively, compared to the compensation model that only considered the sensor subject distance.

To evaluate the end-to-end accuracy of a non-invasive facial temperature screening system, sensitivity in Equation 3 and specificity in Equation 4 were employed. The dataset for conducting the analysis consists of data from the non-fever group and the fever group of calibration data. The cut-off value for fever detection before and after temperature compensation was determined to be 33.8°C and 37.5°C , respectively. The rationale for selecting 33.8°C as the benchmark was based on the Hong Kong Center for Health Protection's Monitoring of Body Temperature Guidance Note [1], which establishes 35.5°C as the fever detection threshold for a FLIR A310 / A315 thermal infrared camera. A

1.7°C difference is revealed in [6] between the FLIR A315 thermal imaging camera and the FLIR E8xt thermal imaging camera. Given that the FLIR E6 and FLIR E8xt share the same hardware, it is reasonable to assume that the temperature difference between the FLIR A315 and the FLIR E6 utilized in the present study is similar between the FLIR A315 and FLIR E8xt.

Figure 8 shows the sensitivity and specificity analysis of four different cases: (i) without temperature compensation, (ii) with the ambient temperature only compensation model, (iii) with distance only compensation model, and (iv) with our proposed compensation model. We defined the valid detection distance as the furthest distance where the system can detect feverish with sensitivity and specificity both

larger than 90%. Since most of the data exceeded the temperature range recommended by the Food and Drug Administration, we chose to use a temperature of 28.8°C for the calibration data. Without compensation, the sensitivity was greater than 90% within 2 m to 6 m using calibration data taken at the ambient temperature of 28.8°C (plus and minus 0.1°C). However, specificity remained consistently zero, indicating that the system is ineffective when the ambient temperature exceeds 24°C, consistent with FDA guidelines [13]. With ambient temperature only compensation model [17], the specificity remained above 90% while sensitivity dropped to lower than 90% after 4.1 m and became 0 at 6 m. In terms of the compensation model only with distance, the specificity still kept larger than 90% between 2 m to 6 m, while the sensitivity fell below 90% after 5.4 m and reached 75% at 6 m. Under the same condition, our proposed compensation model achieved both sensitivity and specificity of larger than 90% from 2 m to 6 m, where 6 m is the physical limit of the site. Regarding valid detection distances, the system with ambient temperature only compensation model, system with distance only compensation model, and system with our proposed compensation model achieved 4.1 m, 5.4 m, and 6 m respectively. Our proposed compensation increased the valid detection distances by 46% and 11% with respect to ambient temperature only compensation model and distance only compensation model. To summarize, our results showed that the facial temperature screening system with temperature compensation enables fever screening outside of the FDA-suggested ambient temperature range. Our solution surpassed the previous works.

5. Conclusions

This paper reports the interaction effects between sensor-subject distance and ambient temperature on the remotely measured facial temperature in a sheltered outdoor site. The result indicates a significant correlation between the measured facial temperature and the ambient temperature ($p < 0.01$: from 15.9°C to 34.4°C, humidity controlled between 60% and 80%), as well as a significant interaction between the effects of ambient temperature and sensor-subject distance ($p < 0.01$: 0.25 m to 6 m) on the measured temperature. Furthermore, we propose a temperature compensation model that significantly reduced the average MAE from 2.5°C to 1.3°C and lowered the average RMSE from 3.3°C to 1.9°C. Using calibration data taken at the ambient temperature of 28.8°C (plus and minus 0.1°C), our proposed model increased the specificity from 0 to 100% compared to without compensation. Similarly, our model achieved a sensitivity of 100% in the range of 2 m to 6 m. These sensitivity results are better than past work that compensates for the influence of ambient temperature only (0%, [17]); and the influence of distance only (75%, [7]). Furthermore,

our model increased the valid detection distance to 6 m (4.1 m [17]; 5.4 m [7]). Without compensation, fever detection does not work under varying ambient temperatures.

6. Future work

Future work involves exploring and compensating for the effect of other factors on temperature measurement, such as humidity, wind, and face orientation. In addition, it would be interesting to study the feasibility of using lateral facial temperature for fever screening as this would increase the flexibility of setting up the fever screening system at different locations and still achieve high detection accuracy.

References

- [1] Infection control branch guidance note on monitoring of body temperature. 7
- [2] David Bell. Public health interventions and sars spread, 2003. *Emerging infectious diseases*, 10:1900–6, 12 2004. 1
- [3] Zhe Cao, Gines Hidalgo, Tomas Simon, Shih-En Wei, and Yaser Sheikh. Openpose: Realtime multi-person 2d pose estimation using part affinity fields. *IEEE transactions on pattern analysis and machine intelligence*, 43(1):172–186, Jan 01, 2021. 2, 4
- [4] B. M. Y. Cheung, L. S. Chan, I. J. Lauder, and C. R. Kumana. Detection of body temperature with infrared thermography: accuracy in detection of fever. *Hong Kong medical journal* 61; *Xianggang yi xue za zhi*, 18 Suppl 3:31–34, Aug 2012. 2
- [5] Ming-Fu Chiang, Po-Wei Lin, Li-Fong Lin, Hung-Yi Chiou, Ching-Wen Chien, Shu-Fen Chu, and Wen-Ta Chiu. Mass screening of suspected febrile patients with remote-sensing infrared thermography: Alarm temperature and optimal distance. *Journal of the Formosan Medical Association*, 107(12):937–944, 2008. 1
- [6] Jing Wei Chin. Online decision analytics with deep learning : non-invasive fever screening. 7
- [7] Jing Wei Chin, Kwan Long Wong, Tsz Tai Chan, Kristian Suhartono, and Richard H. Y. So. An infrared thermography model enabling remote body temperature screening up to 10 meters. pages 3870–3876. *IEEE*, Jun 2021. 2, 3, 5, 8
- [8] Gabriel Cruz, Raul Mamani, Henry Torres, Victor Salcedo, Cristian Benites, Reencarnacion Quispe, Franklin Cardeñoso, and Jorge L. Arizaca-Cusicuna. Evaluation of adjustment models for taking body temperature with a thermal imaging camera in the context of covid-19, -07-20 2022. 2
- [9] Yu cun Zhang, Yi ming Chen, Xian bin Fu, and Cheng Luo. A method for reducing the influence of measuring distance on infrared thermal imager temperature measurement accuracy. *Applied thermal engineering*, 100:1095–1101, May 05, 2016. 2
- [10] Kaiyuan Hou, Yan Chen Liu, Peter Wei, Chenye Yang, Hengjiu Kang, Stephen Xia, Teresa Spada, Andrew Rundle, and Xiaofan Jiang. A low-cost in-situ system for continuous

- multi-person fever screening. In *2022 21st ACM/IEEE International Conference on Information Processing in Sensor Networks (IPSN)*, pages 15–27, 2022. 2
- [11] B.B. Lahiri, S. Bagavathiappan, T. Jayakumar, and John Philip. Medical applications of infrared thermography: A review. *Infrared Physics Technology*, 55(4):221–235, 2012. 2
- [12] Eddie Yk Ng and Mahnaz EtehadTavakol. *Applications of Infrared Thermography for Noncontact and Noninvasive Mass Screening of Febrile International Travelers at Airport Quarantine Stations*, pages 347–358. Application of Infrared to Biomedical Sciences. Springer Singapore Pte. Limited, Singapore, Jan 01, 2017. 2
- [13] Ogre Development Team. Thermal imaging systems (infrared thermographic systems / thermal imaging cameras). <https://www.fda.gov/medical-devices/general-hospital-devices-and-supplies/thermal-imaging-systems-infrared-thermographic-systems-thermal-imaging-cameras>, 2019. 1, 5, 8
- [14] Dong Pan, Zhaohui Jiang, Weihua Gui, Xavier Maldague, and Ke Jiang. Influence of dust on temperature measurement using infrared thermal imager. *IEEE Sensors Journal*, 20(6):2911–2918, 2020. 2
- [15] Patricia C. Priest, Alasdair R. Duncan, Lance C. Jennings, and Michael G. Baker. Thermal image scanning for influenza border screening: Results of an airport screening study. *PLoS ONE*, 6(1):e14490, Jan 05, 2011. 2
- [16] Kunal Rao, Giuseppe Coviello, Min Feng, Biplob Debnath, Wang-Pin Hsiung, Murugan Sankaradas, Yi Yang, Oliver Po, Utsav Drolia, and Srimat Chakradhar. F3s: Free flow fever screening. pages 276–285, Ithaca, Aug 2021. IEEE. 2
- [17] Sirajit Rayanasukha, Armote Somboonkaew, Sarun Sumridetchkajorn, Kosom Chaitavon, Sataporn Chanhorm, Bunpot Saekow, and Supanit Porntheeraphat. Self-compensation for the influence of working distance and ambient temperature on thermal imaging-based temperature measurement. *IEEE transactions on instrumentation and measurement*, 70:1–6, 2021. 2, 8
- [18] Joseph Redmon, Santosh Divvala, Ross Girshick, and Ali Farhadi. You only look once: Unified, real-time object detection, 2015. 2
- [19] Adrian Shajkofci. Correction of human forehead temperature variations measured by non-contact infrared thermometer. *IEEE Sensors Journal*, 22(17):16750–16755, 2022. 2
- [20] Guanghao Sun, Takemi Matsui, Tetsuo Kirimoto, Yu Yao, and Shigeto Abe. Applications of infrared thermography for noncontact and noninvasive mass screening of febrile international travelers at airport quarantine stations, -03 2017. 1, 2
- [21] M. R. Tay, Y. L. Low, X. Zhao, A. R. Cook, and V. J. Lee. Comparison of infrared thermal detection systems for mass fever screening in a tropical healthcare setting. *Public Health*, 129(11):1471–1478, 2015. 2
- [22] Pauli Virtanen, Ralf Gommers, Travis E. Oliphant, Matt Haberland, Tyler Reddy, David Cournapeau, Evgeni Burovski, Pearu Peterson, Warren Weckesser, Jonathan Bright, Stéfan J. van der Walt, Matthew Brett, Joshua Wilson, K. Jarrod Millman, Nikolay Mayorov, Andrew R. J. Nelson, Eric Jones, Robert Kern, Eric Larson, C J Carey, İlhan Polat, Yu Feng, Eric W. Moore, Jake VanderPlas, Denis Laxalde, Josef Perktold, Robert Cimrman, Ian Henriksen, E. A. Quintero, Charles R. Harris, Anne M. Archibald, Antônio H. Ribeiro, Fabian Pedregosa, Paul van Mulbregt, and SciPy 1.0 Contributors. SciPy 1.0: Fundamental Algorithms for Scientific Computing in Python. *Nature Methods*, 17:261–272, 2020. 6
- [23] Quanxing Wan, Benjamin Brede, Magdalena Smigaj, and Lammert Kooistra. Factors influencing temperature measurements from miniaturized thermal infrared (tir) cameras: A laboratory-based approach. *Sensors (Basel, Switzerland)*, 21(24):8466, 2021. 2, 6
- [24] Yangling Zhou, Pejman Ghassemi, Michelle Chen, David McBride, Jon P. Casamento, T. Joshua Pfefer, and Quanzeng Wang. Clinical evaluation of fever-screening thermography: impact of consensus guidelines and facial measurement location, -09 2020. 3